Graded-index optical dimer formed by optical force

Alireza Akbarzadeh,[1,*] Thomas Koschny,[2] Maria Kafesaki,[1,3] Eleftherios N. Economou,[1] and Costas M. Soukoulis[1,2]

[1]*Institute of Electronic Structure and Laser, Foundation for Research & Technology-Hellas, Heraklion, Crete, 71110, Greece*
[2]*Ames Laboratory and Department of Physics and Astronomy, Iowa State University, Ames, Iowa, 50011, USA*
[3]*Department of Materials Science and Technology, University of Crete, Heraklion, 71003, Greece*
[*]*alireza.akbarzadeh@iesl.forth.gr*

Abstract: We propose an optical dimer formed from two spherical lenses bound by the pressure that light exerts on matter. With the help of the method of force tracing, we find the required graded-index profiles of the lenses for the existence of the dimer. We study the dynamics of the opto-mechanical interaction of lenses under the illumination of collimated light beams and quantitatively validate the performance of proposed dimer. We also examine the stability of dimer due to the lateral misalignments and we show how restoring forces bring the dimer into lateral equilibrium. The dimer can be employed in various practical applications such as optical manipulation, sensing and imaging.

OCIS codes: (350.4855) Optical tweezers or optical manipulation; (160.2710) Inhomogeneous optical media; (080.0080) Geometric optics; (120.4880) Optomechanics.

References and links

1. J. C. Maxwell, *A Treatise on Electricity and Magnetism* (Clarendon, 1904).
2. A. Bartoli, "Il calorico raggiante e il secondo principio di termodinamica," Nuovo Cim. **15**(1), 193–202 (1884).
3. P. N. Lebedev, "Investigations on the pressure forces of light," Ann. Phys. **6**, 433–458 (1901).
4. E. F. Nichols and G. F. Hull, "The pressure due to radiation (Second paper)," Phys. Rev. **17**, 26–50 (1903).
5. E. F. Nichols and G. F. Hull, "The pressure due to radiation," Astrophys. J. **57**, 315–351 (1903).
6. I. Brevik, "Experiments in phenomenological electrodynamics and the electromagnetic energy-momentum tensor," Phys. Rep. **52**(3), 133–201 (1979).
7. U. Leonhardt, "Optics: momentum in an uncertain light," Nature **444**(7121), 823–824 (2006).
8. R. N. C. Pfeifer, T. A. Nieminen, N. R. Heckenberg, and H. Rubinsztein-Dunlop, "Colloquium: momentum of an electromagnetic wave in dielectric media," Rev. Mod. Phys. **79**(4), 1197–1216 (2007).
9. B. Kemp, T. Grzegorczyk, and J. Kong, "Ab initio study of the radiation pressure on dielectric and magnetic media," Opt. Express **13**(23), 9280–9291 (2005).
10. M. Nieto-Vesperinas, J. J. Sáenz, R. Gómez-Medina, and L. Chantada, "Optical forces on small magnetodielectric particles," Opt. Express **18**(11), 11428–11443 (2010).
11. A. Ashkin, "Acceleration and trapping of particles by radiation pressure," Phys. Rev. Lett. **24**(4), 156–159 (1970).
12. A. Ashkin, J. M. Dziedzic, J. E. Bjorkholm, and S. Chu, "Observation of a single-beam gradient force optical trap for dielectric particles," Opt. Lett. **11**(5), 288–290 (1986).
13. D. G. Grier, "A revolution in optical manipulation," Nature **424**(6950), 810–816 (2003).
14. T. J. Kippenberg and K. J. Vahala, "Cavity optomechanics: back-action at the mesoscale," Science **321**(5893), 1172–1176 (2008).
15. M. Aspelmeyer, T. J. Kippenberg, and F. Marquardt, "Cavity optomechanics," Rev. Mod. Phys. **86**(4), 1391–1452 (2014).
16. H. J. Metcalf and P. van der Straten, *Laser Cooling and Trapping* (Springer, 1999).
17. K. Svoboda and S. M. Block, "Biological applications of optical forces," Annu. Rev. Biophys. Biomol. Struct. **23**(1), 247–285 (1994).
18. K. C. Neuman and A. Nagy, "Single-molecule force spectroscopy: optical tweezers, magnetic tweezers and atomic force microscopy," Nat. Methods **5**(6), 491–505 (2008).
19. M. Liu, T. Zentgraf, Y. Liu, G. Bartal, and X. Zhang, "Light-driven nanoscale plasmonic motors," Nat. Nanotechnol. **5**(8), 570–573 (2010).
20. J. Chen, J. Ng, Z. Lin, and C. T. Chan, "Optical pulling force," Nat. Photonics **5**(9), 531–534 (2011).
21. A. Novitsky, C. W. Qiu, and H. Wang, "Single gradientless light beam drags particles as tractor beams," Phys. Rev. Lett. **107**(20), 203601 (2011).

#260902 Received 10 Mar 2016; revised 13 Apr 2016; accepted 13 Apr 2016; published 17 May 2016

22. D. B. Ruffner and D. G. Grier, "Optical conveyors: a class of active tractor beams," Phys. Rev. Lett. **109**(16), 163903 (2012).
23. O. Brzobohatý, V. Karásek, M. Šiler, L. Chvátal, T. Čižmár, and P. Zemánek, "Experimental demonstration of optical transport, sorting and self-arrangement using a 'tractor beam'," Nat. Photonics **7**(2), 123–127 (2013).
24. V. Kajorndejnuku, W. Ding, S. Sukhov, C.-W. Qiu, and A. Dogariu, "Linear momentum increases and negative optical forces at dielectric interface," Nat. Photonics **7**(10), 787–790 (2013).
25. H. Chen, B. Zhang, Y. Luo, B. A. Kemp, J. Zhang, L. Ran, and B. Wu, "Lorentz force and radiation pressure on a spherical cloak," Phys. Rev. A **80**(1), 011808 (2009).
26. H. Chen, B. Zhang, B. A. Kemp, and B. I. Wu, "Optical force on a cylindrical cloak under arbitrary wave illumination," Opt. Lett. **35**(5), 667–669 (2010).
27. P. C. Chaumet, A. Rahmani, F. Zolla, A. Nicolet, and K. Belkebir, "Optical force on a discrete invisibility cloak in time-independent fields," Phys. Rev. A **84**(3), 033808 (2011).
28. P. C. Chaumet, A. Rahmani, F. Zolla, and A. Nicolet, "Electromagnetic forces on a discrete spherical invisibility cloak under time-harmonic illumination," Phys. Rev. E Stat. Nonlin. Soft Matter Phys. **85**(5), 056602 (2012).
29. J. D. Jackson, *Classical Electrodynamics* (John Wiley, 1998).
30. J. A. Kong, *Electromagnetic Wave Theory* (Wiley, 1986).
31. A. Akbarzadeh, M. Danesh, C. W. Qiu, and A. J. Danner, "Tracing optical force fields within graded-index media," New J. Phys. **16**(5), 053035 (2014).
32. A. Akbarzadeh, J. A. Crosse, M. Danesh, C. W. Qiu, A. J. Danner, and C. M. Soukoulis, "Interplay of optical force and ray-optic behavior between Luneburg lenses," ACS Photonics **2**(9), 1384–1390 (2015).
33. U. Leonhardt and T. G. Philbin, *Geometry and Light: The Science of Invisibility* (Dover, 2010).
34. A. Akbarzadeh and A. J. Danner, "Generalization of ray tracing in a linear inhomogeneous anisotropic medium: a coordinate-free approach," J. Opt. Soc. Am. A **27**(12), 2558–2562 (2010).
35. A. J. Danner, "Singularity removal in optical instruments without reflections or induced birefringence," New J. Phys. **12**(11), 113008 (2010).

1. Introduction

In 1891 Maxwell predicted an observable mechanical effect due to light rays falling on a suspended disc and the concept of optical forces and the momentum of light appeared in its modern form [1]. Concurrently, based on the second law of thermodynamics, a similar conclusion was made by Bartoli [2]. These early theoretical predictions were validated in several experiments conducted by Lebedev, Nichols and Hull [3–5]. Since then, the momentum that light carries and its mechanical interaction with media has been under intensive scrutiny and many different aspects of the electrodynamics of light-matter interaction have been studied [6–10]. On the basis of these studies, many practical applications for this opto-mechanical effect have been proposed and realized. For example, the pioneering work of Arthur Ashkin and his colleagues on particle trapping, led to the development of optical tweezer, a methodology that has revolutionized many areas of science and technology [11–13]. Cavity optomechanics and cooling [14–16], microscopy and optical imaging [17, 18], the driving of nanoscale motors with light [19], tractor beams [20–24], and the radiation pressure on invisibility cloaks [25–28] are few modern applications of optical forces.

The standard approach to calculating the optical force is to integrate the divergence of stress tensor - which is constructed from the electromagnetic fields - over the volume of interest [29, 30]. Nevertheless, this procedure is not always straightforward and it often requires time-consuming computations. In Ref [31]. the language of geometrical optics was used to simplify the computational complexities of the standard procedure. This method, which is known as force tracing, uses geometric optics expressions to calculate the optical force field along the trajectories of light rays in a medium. Subsequently, in another paper [32] the method of force tracing was applied to investigate the mechanical collision of Luneburg lenses under the illumination of collimated light beams and its potential applications in optical manipulation.

Following on from these two previous works, we, here, use the force tracing technique to design an optical dimer constructed from two graded-index lenses [see Fig. 1(a)]. We use the optical force to bond the lenses and cancel the gravitational force. We find that one of the lenses should be a conventional Luneburg lens [33] and the other a modified Luneburg lens, which we will refer to as pseudo Luneburg lens. Using the force tracing technique to study the dynamics of these lenses when illuminated by collimated light rays we demonstrate how the dimer can be constructed. We also study the stability of the system and examine its

#260902 Received 10 Mar 2016; revised 13 Apr 2016; accepted 13 Apr 2016; published 17 May 2016

sensitivity to the possible misalignment. We show that the proposed dimer is stable and the arising optical lateral forces compensate for any misalignment, bringing the lenses into alignment with the illuminating light beam. The resulting optical dimer is a versatile device which can offer an appropriate platform for various applications such as sensing, particle imaging and optical manipulation.

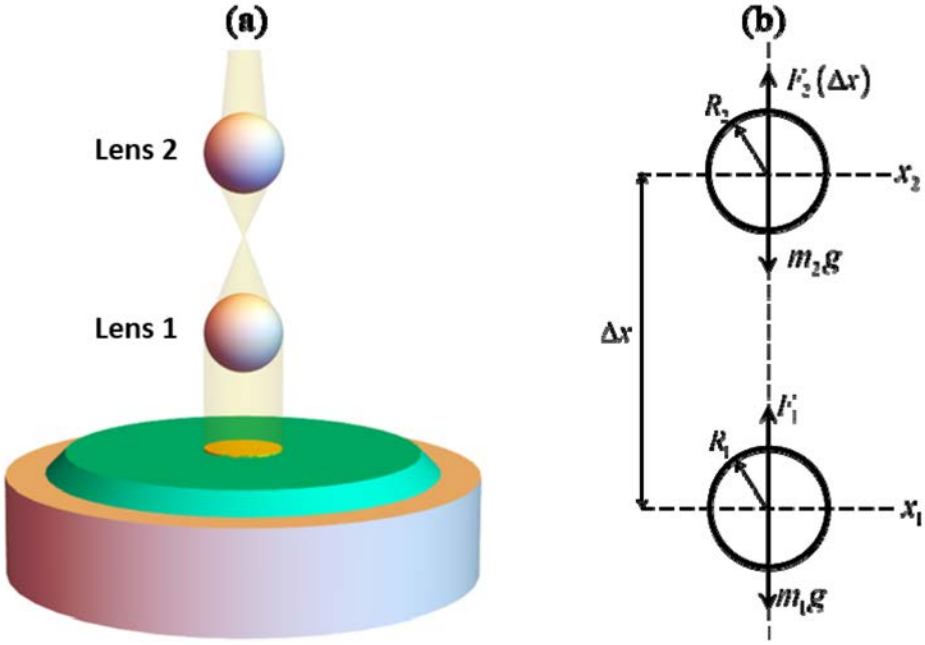

Fig. 1. (a) 3D schematic of the proposed dimer under the illumination by a collimated light beam. (b) The geometry of the suggested dimer (for parameter definitions see main text).

2. A brief review of force tracing

The method of force tracing introduced in [31] is based on an approximate formulation which is valid in the realm of geometrical optics. In this regime, the electromagnetic fields are taken as the quasi-plane waves with rapidly varying phases and slowly varying amplitudes,

$$\begin{cases} \vec{E}(\vec{r},t) = \vec{E}_0 \exp\left(ik_0\vec{k}\cdot\vec{r} - i\omega t\right) \\ \vec{H}(\vec{r},t) = \vec{H}_0 \exp\left(ik_0\vec{k}\cdot\vec{r} - i\omega t\right) \end{cases} \tag{1}$$

where ω is the angular frequency, $\vec{k}$ is the wave vector, $k_0 = \omega/c$, c is the speed of light in vacuum, and $\vec{E}_0$ and $\vec{H}_0$ are vectors with approximately constant amplitudes. Taking the above expressions for the electromagnetic fields and employing the Hamiltonian-based ray formulation [33, 34] assisted by the appropriate constitutive equations, the Lorentz force density in a spherically symmetric isotropic medium simplifies to [31],

#260902 Received 10 Mar 2016; revised 13 Apr 2016; accepted 13 Apr 2016; published 17 May 2016

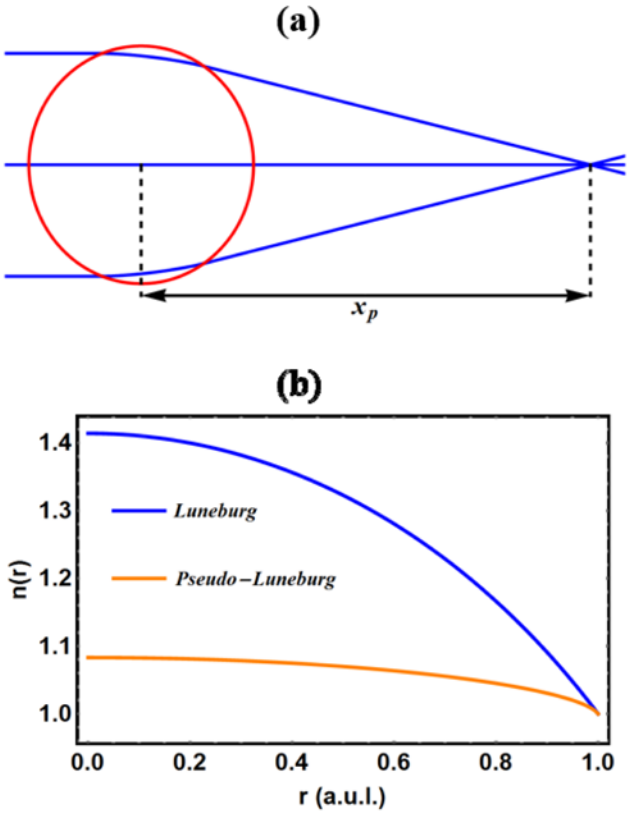

Fig. 2. (a) The ray tracing of the pseudo Luneburg lens. (b) The profile index of the pseudo Luneburg lens for $x_p = 4R_1$ compared to the profile index of conventional Luneburg lens ($R_1 = R_2 = 1$a.u.l.).

$$\left\langle \vec{f} \right\rangle_{normalized} = \frac{2b}{rn(r)^3} \frac{dn}{dr} \left(\vec{k} \times \hat{e}_n \right) \tag{2}$$

where b is the impact parameter of the incident ray, $\hat{e}_n$ is the unit vector normal to the plane of rays, and $n(r)$ is the graded-index profile of corresponding medium. It should be noted that in Eq. (2) the obtained Lorentz force density is normalized with respect to $\varepsilon_0 \left| \vec{E}_0 \right|^2 / 2$, in which ε_0 is the permittivity of free space. In Ref [31]. it was shown that the magnitude of normalized Lorentz force density in a generalized isotropic medium is directly proportional to the curvature of traced ray trajectories. In other words, the more sharply the rays bend in the medium, the stronger the opto-mechanical interaction. By applying the force tracing method on several example optical devices and comparing the obtained results with those of the full-wave analyses, the authors of Ref [31]. confirmed the validity of the formulation. Nonetheless, the expressions for anisotropic media given in Ref [31]. are only true for the diagonal constitutive tensors and they should be modified for non-diagonal cases.

Using the force tracing mehod, it is easy to show that a collimated light beam applies a positive force on a Luneburg lens, pushing it in the direction of propagation. Conversely, light rays entering a Luneburg lens from a single point exert a negative force on the lens. In other words, if the separation between two neighboring Luneburg lenses is small enough, the light

#260902 Received 10 Mar 2016; revised 13 Apr 2016; accepted 13 Apr 2016; published 17 May 2016

will cause an attractive force between them. This effect was investigated in Ref [32]. for both elastic and fully inelastic collisions. It was shown that the two lenses exhibit simultaneous oscillatory and translational motion and undergo an infinite series of collisions. However, in a realistic situation the presence of dissipation affects the motion of lenses and damps the amplitude of the oscillations. It was also discussed in Ref [32]. how the radiation pressure can combine two and four Luneburg lenses in ways which are useful for various types of optical manipulation.

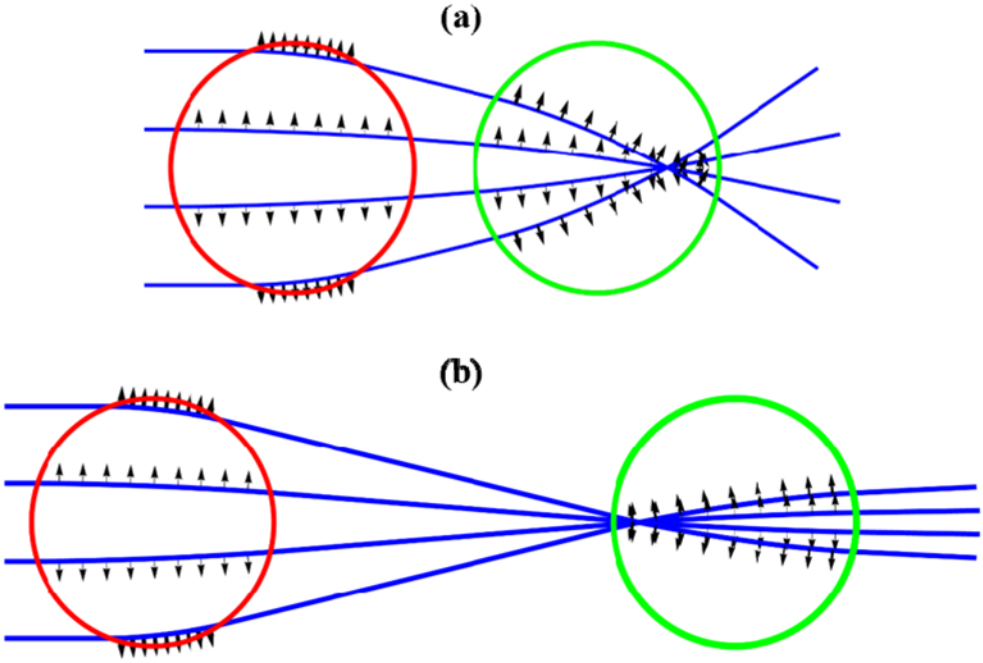

Fig. 3. The force fields applied on the combination of a pseudo Luneburg lens with $x_p = 4R_1$ (the red lens) and a Luneburg lens (the green lens) induced by the light rays propagating from the left for (a) $\Delta x = 1.25R$ (repulsion), and (b) $\Delta x = 2.4R$ (attraction).

3. The dimer design

Here, we design a dimer formed from two spherically symmetric lenses. The lenses should be bonded together without contact while the whole system is suspended by an upward optical force balancing the downward effects of gravity. The system of two Luneburg lenses in Ref [32]. under the illumination of collimated light beam exhibit translational and oscillatory motion and the lenses experience a series of collisions until dissipation effects damp away the oscillations such that the lenses remain in continuous contact. The analysis in Ref [32]. shows that the force on the second lens is negative (attractive) when the lenses are close to each other. This force becomes positive (repulsive) when the second lens is far enough from the first one. In other words, the second lens experiences a potential well due to its interaction with the first lens. This potential well is the origin of collisions and the reason why the system with lenses at a non-zero separation in unstable. Due to the unwanted collisions and the seperational instability, the system of two Luneburg lenses is not an appropriate choice for making the dimer. In designing the dimer we need to engineer a potential that results in a stable non-zero separation between the lenses. This implies that the force on the second lens should be positive in the vicinity of the first one. Then, as the second lens gets farther away, the exerted force should decrease until it reaches negative values. However, the force cannot remain negative and after reaching a local minimum it should tend toward the positive values.

#260902 Received 10 Mar 2016; revised 13 Apr 2016; accepted 13 Apr 2016; published 17 May 2016

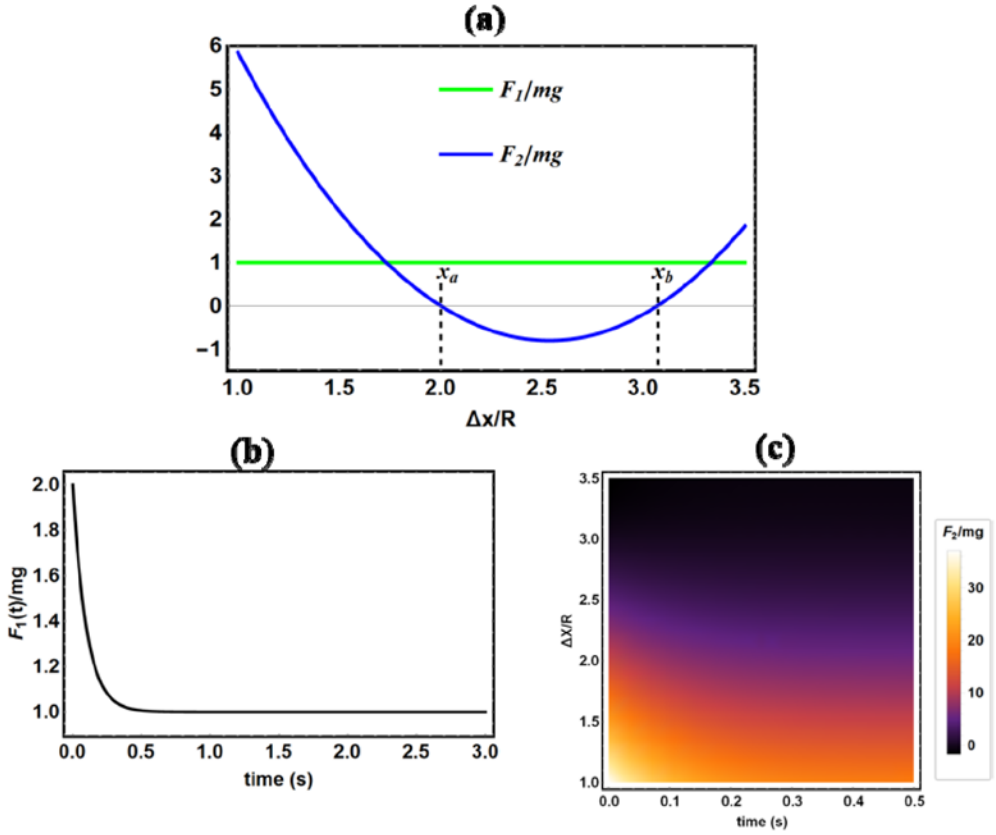

Fig. 4. (a) The forces applied on the pseudo Luneburg lens (F_1) and the Luneburg lens (F_2), as a function of the distance between the lenses. Note that F_2 is zero at points $x = x_a$ and $x = x_b$. (b) Temporal variation of F_1 due to the fluctuation of incident light intensity over time. (c) The density plot of F_2 versus time and the separation between the lenses.

Let us assume that the second lens in the dimer is a Luneburg lens. Given this assumption, the minimum negative force on the second lens occurs at the focal point of the first lens. Moreover, in order for the second lens to feel a positive force at short separation distances, the first lens should deflect the incoming rays less than the Luneburg lens. These two criteria show that the first lens should be a modified version of Luneburg lens (pseudo Luneburg lens) with the focal point somewhere outside the lens ($x_p > R_1$). In order to obtain the profile index of pseudo Luneburg lens, we first determine the turning angles of rays $\chi(b)$ toward the origin of lens as a function of the impact parameter and then solve the following implicit integral equation for $n(r)$ [35],

$$n(r) = \exp\left(\frac{1}{\pi}\int_{R_1\rho}^{R_1} \frac{\chi(b)\,db}{r\sqrt{b^2/r^2-\rho^2}}\right) \tag{3}$$

#260902 Received 10 Mar 2016; revised 13 Apr 2016; accepted 13 Apr 2016; published 17 May 2016

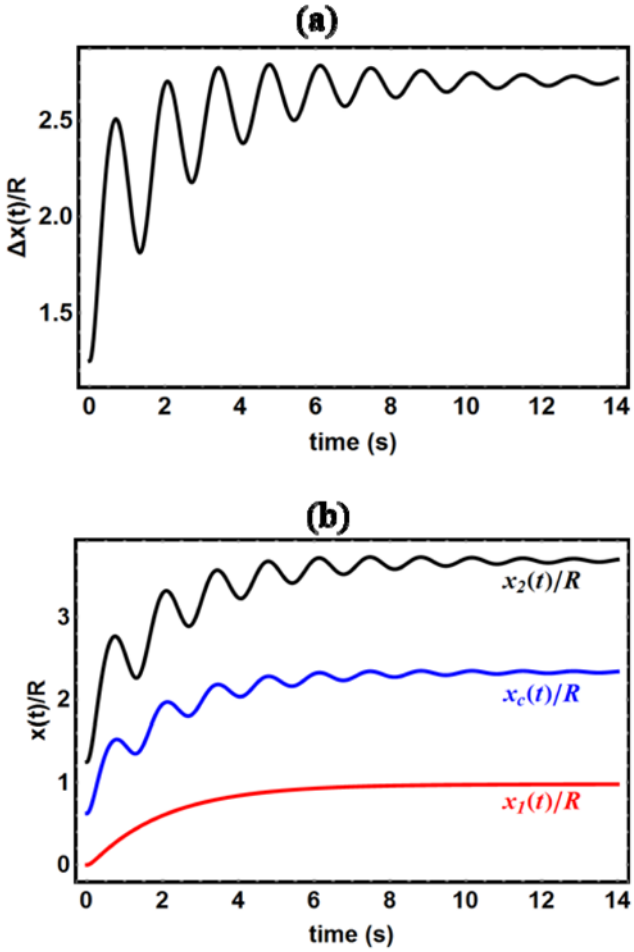

Fig. 5. (a) The separation between the lenses vs time. (b) The paths of the two lenses and the corresponding center of mass vs time for $\Delta x_0 = 1.25R$, $k_d = 0.5\mathrm{s}^{-1}$. (see Visualization 1)

where $\rho = rn(r)/R_1$ and R_1 is the radius of the lens, which is equal to 1 in arbitrary units of length (a.u.l.) for the current case. Note that for a specific range of wavelengths the a.u.l. should be chosen such that the radii of lenses are always larger than the wavelength of incident beam and also, the variations of the profile indices in that range of wavelengths remain negligible. The profile index and ray trajectories of a pseudo Luneburg lens with the focal point $x_p = 4R_1$ are shown in Fig. 2. After recognizing the functionality of lenses, we proceed to demonstrate how the system of the two lenses functions as a dimer. We apply the method of force tracing to obtain the force fields within the lenses. Then with the obtained force profiles we formulate the dynamics of the interaction between the lenses and calculate the corresponding equations of motion.

In order to find the force profiles inside the lenses, we perform the ray tracing with respect to the refractive indices and the geometrical boundaries in the whole domain of interest. Then, with the use of Eq. (2), we trace the force fields along the ray trajectories. The results of the force tracing analysis are shown in Fig. 3. As seen in Fig. 3, all the incoming rays enter the pseudo Luneburg lens in parallel and hence a constant positive force is always exerted on the pseudo Luneburg lens. However, compared to the Luneburg lens, the curvatures of rays in the pseudo Luneburg lens are smaller and hence the magnitude of applied force on the pseudo

#260902 Received 10 Mar 2016; revised 13 Apr 2016; accepted 13 Apr 2016; published 17 May 2016

Luneburg lens is also smaller. The force acting on the second lens in the dimer is dependent on its distance from the first lens. In the vicinity of first lens the force on the second lens is positive and as the distance between the lenses increases, the force on the second lens decreases monotonically so that it becomes negative. After reaching a local minimum this force increases toward the positive values again. This trend can be seen in Fig. 4, where the approximate total force acting on the two lenses versus the distance between them is shown. In order to find this approximate total force we integrate the force density along rays all over the lenses as $\left\langle \vec{F} \right\rangle_{normalized} = \int \left\langle \vec{f}\left(\vec{r}\left(\tau\right)\right) \right\rangle_{normalized} n\left(\vec{r}\left(\tau\right)\right) d\tau$, where τ is the ray tracing parameter [31].

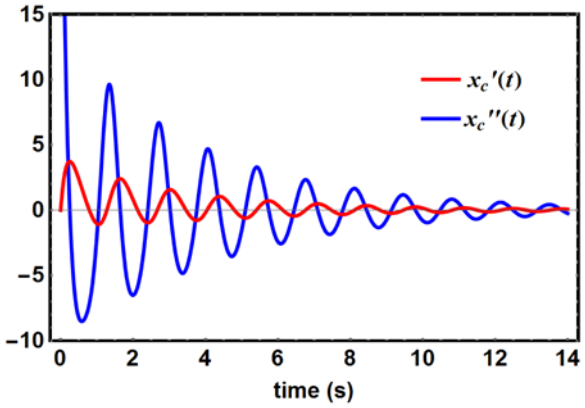

Fig. 6. The velocity $x_c'\left(t\right)$ (a.u.l./s) and the acceleration $x_c''\left(t\right)$ (a.u.l./s^2) of the center of mass of dimer vs time.

In order to study the dynamics of opto-mechanical interaction between the lenses, we assume they have identical masses $m_1 = m_2 = m$ and radii $R_1 = R_2 = R/2$ [see Fig. 1(b)]. As indicated in Fig. 4(a), we assume that the force on the first lens is independent of its position, i.e. $F_1\left(x_1\right) = F_1$, and the force on the second lens is subject to its distance from the first lens, i.e. $F_2 = F_2\left(\Delta x\right)$ with $\Delta x = x_2 - x_1$. Then the equations of motion for the first lens x_1 and the separation Δx are,

$$\frac{d^2 x_1}{dt^2} + k_d \frac{dx_1}{dt} = \frac{F_1}{m} - g \tag{4}$$

$$\frac{d^2 \Delta x}{dt^2} = \frac{d^2 x_2}{dt^2} - \frac{d^2 x_1}{dt^2} = \frac{F_2 - F_1}{m} - k_d \frac{d\Delta x}{dt} \tag{5}$$

where $g \approx 9.8\,\mathrm{m/s^2}$ is the acceleration of gravity and k_d is the damping factor. In order to study the dynamics of the system in a more realistic situation, we assume that the intensity of illuminating beam changes with respect to time and, as shown in Fig. 4(b), the force on the first lens gradually approaches the gravitational force (i.e. $F_1 = F_1\left(t\right)$). Note that $F_1\left(t\right)$ is directly proportional to the intensity of incident light and the intensity of incident beam has a time dependence similar to that shown in Fig. 4(b). Consequently, as shown in Fig. 4(c), the forces on the second lens is also time-varying, i.e. $F_2 = F_2\left(\Delta x, t\right)$. With the use of the given force profiles, we solve the equations of motion and the obtained numerical results are presented in Fig. 5. The two lenses initially are at rest and located at a distance like Δx_0 from each other. The time dependence of the separation parameter behaves like a damped

#260902 Received 10 Mar 2016; revised 13 Apr 2016; accepted 13 Apr 2016; published 17 May 2016

oscillatory function superimposed on a sigmoidal curve. As implied from Fig. 5(b) and verified in Fig. 6, as soon as the beam is turned on, the two lenses accelerate and, depending on the influence of the existing forces, exhibit translational and/or oscillatory motion. However, the oscillatory and translational motions are damped away after an initial transient stage and the lenses asymptotically reach equilibrium, at which they will be suspended steadily.

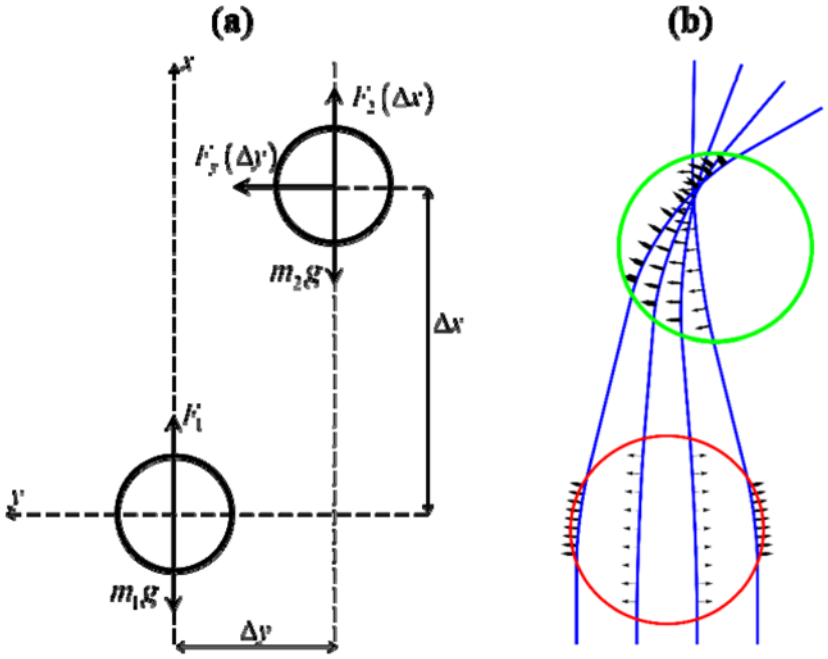

Fig. 7. (a) The geometry of dimer with the lateral misalignment under the illumination of collimated light rays. (b) The force fields on the lenses as a result of light rays shining from below ($\Delta y = -0.25R$).

The oscillatory and translational motion of system is affected by several parameters such as the initial separation Δx_0, the damping factor k_d, the initial acceleration of the lenses and the time-dependence of incident light beam. The damping factor influences the speed of the lenses and their final suspending positions. As the damping factor of system grows, the translational motions of lenses vanish faster, i.e. the corresponding sigmoidal curves converge to their asymptotes in a shorter time. The damping factor also affects the oscillations of second lens - the larger the damping factor the smaller the amplitudes of the oscillations. The other parameter which determines the final position of second lens and its oscillations is the initial separation between the lenses. Depending on the initial position of lenses, the response function of dimer varies. In fact, if the initial separation Δx_0 is close to a value like Δx_{0opt}, for which we have $F_2\left(\Delta x_{0opt}, 0\right) - F_1\left(0\right) \approx 0$, then the amplitudes of oscillations would be minimized and the motion of system would be mostly translational. It is also obvious that in order for the dimer to work correctly, the initial position of second lens $x_{2,0}$ should be before the second zero of $F_2\left(\Delta x, 0\right)$, i.e. $R < x_{2,0} < x_b$ [see Fig. 4(a)]. The initial acceleration imposed on the lenses and the intensity variation of incident light beam with respect to time determines the duration of the transient stage (i.e. the steepness of the sigmoidal curve) as well as the location of the final suspending points (i.e. the asymptotes). A clearer understanding of the motion of the lenses can be gained if we investigate the motion of the

#260902 Received 10 Mar 2016; revised 13 Apr 2016; accepted 13 Apr 2016; published 17 May 2016

center of mass $x_c = x_1 + \Delta x/2$. As shown in Fig. 6, the incident light induces an initial acceleration on the center of mass in the direction of propagation of the light. However, this acceleration decreases over time and at the moment of maximum forward speed a force in the direction opposite to the direction of light propagation is induced, decelerating the center of mass. Likewise, after a period of time, the deceleration is replaced by another acceleration. The sequence of acceleration and deceleration goes on in a damped cyclic manner untill eventually the center of mass stops its motion. Based on the above explanations and the provided figures it is proven that the optical force can cause the considered lenses to float in the space and function as a dimer.

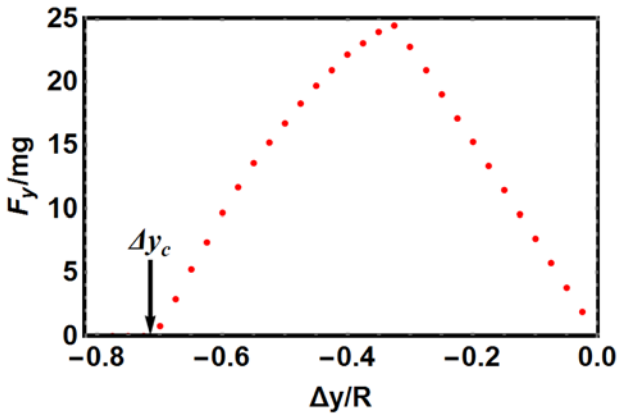

Fig. 8. The restoring force acting on the Luneburg lens vs the lateral misalignment.

A final consideration is the lateral stability of the proposed dimer and its sensitivity to misalignment of lenses, which is likely to occur in practice. In order to examine how the dimer responds to the misalignment, we assume that in addition to the longitudinal separation Δx, there exists a lateral separation Δy between the lenses [see Fig. 7(a)]. Then we apply the force tracing method on the shown setup to study how the lateral forces F_y due to the misalignment may affect the dimer. The result of force tracing analysis are shown in Fig. 7(b). When the lenses are completely aligned along the x axis, i.e. $\Delta y = 0$, owing to the spherical symmetry of lenses the net lateral force acting on each of the lenses is zero. However, if the lenses are not placed along the x axis, then the symmetry of setup around the direction of beam illumination is broken and due to this asymmetry the distribution of rays in the second lens is uneven. For instance, if $\Delta y < 0$ as shown in Fig. 7(b), more rays will enter the left half of the second lens than the right half and, due to the impact parameters and curvatures of corresponding rays, a positive lateral force $F_y > 0$ will be exerted on the second lens. In other words, if the lenses are not positioned along the direction of the incident light rays, a restoring lateral force appears to align the lenses along that direction and bring back the dimer into its equilibrium state. It should be noted that as soon as Δy starts changing from zero, the restoring force emerges and keeps increasing monotonically. However, if Δy is growing beyond a threshold value such as Δy_c, which is related to the focal point of pseudo Luneburg lens, no rays will impinge on the second lens and hence there will be no optical force acting on it. It means that the restoring force must reach its maximum level somewhere between $\Delta y = 0$ and $\Delta y = \Delta y_c$. Figure 8 shows the total lateral force versus the lateral distance between the two lenses. Needless to mention that similar story can be said for the case $\Delta y > 0$. Hence, as long as the lateral distance is smaller than the threshold value, the dimer is able to correct any possible lateral misalignment and, hence, is a stable device.

#260902 Received 10 Mar 2016; revised 13 Apr 2016; accepted 13 Apr 2016; published 17 May 2016

4. Conclusion

In conclusion, we have proposed an optical dimer constructed from a conventional Luneburg lens and a pseudo Luneburg lens, whose profile index was computed with the use of the implicit integral equation. Then we performed the method of force tracing on the two lenses and calculated the optical force fields along the ray trajectories inside the lenses. Based on the obtained force profiles, we studied the dynamics of the opto-mechanical interaction of lenses under the illumination of a collimated light beam and showed how the combination of lenses forms the dimer. We also studied the stability of dimer and we showed that the existence of a restoring force leads to the dimer self-correcting small lateral misalignment. Finally, as a suggestion for the future work we should add that the presented work can constitute a first step towards designing the light-driven alignment and self-aligned optical systems.

Acknowledgments

Work at FORTH was supported by the European Research Council under ERC Advanced Grant No. 320081 (PHOTOMETA). Work at Ames Laboratory was partially supported by the U.S. Department of Energy, Office of Basic Energy Science, Division of Materials Sciences and Engineering, Contract No. DE-AC02-07CH11358.

#260902 Received 10 Mar 2016; revised 13 Apr 2016; accepted 13 Apr 2016; published 17 May 2016